Effects of Polyaminocarboxylate Metal Chelators on Iron-thiolate Induced Oxidation of Methionine- and Histidine-Containing Peptides

Fang Zhao,[1] Jian Yang,[1,2] and Christian Schöneich[1,3]

Received March 8, 1996; accepted March 19, 1996

Purpose. Site-specific protein oxidation induced by prooxidant/metal/oxygen has been recognized as one of the major degradation pathways of protein pharmaceuticals. Polyaminocarboxylate (PAC) metal chelators are commonly employed to prevent metal-catalyzed oxidation, for they sequester metals. However, studies have indicated that iron chelates may still be catalytically active due to their specific coordination geometry. The purpose of this study was to investigate how PAC chelators affect prooxidant/metal/oxygen-catalyzed oxidation of peptides containing histidine (His) and methionine (Met).

Methods. PACs were applied to a model oxidizing system, dithiothreitol/iron/oxygen, which was shown to promote the oxidation of Met to Met sulfoxide in the two model peptides, GGGMGGG and GHGMGGG.

Results. PAC chelators did not suppress the peptide oxidation but significantly changed the product pattern. In particular, the yield of Met sulfoxide dropped significantly, while a number of other products emerged, including oxidation products from the N-terminus and His (if present). Overall, the oxidation became rather non-selective in the presence of PACs. The oxidation kinetics were significantly accelerated by nitrilotriacetate (NTA), ethylenediaminediacetate (EDDA), and ethylenediaminetetraacetate (EDTA), but they were slowed down by ethylenebis(oxyethylenenitrilo)tetraacetate (EGTA) and diethylenetriaminepentaacetate (DTPA). Meanwhile the PAC chelators were also observed to undergo degradation. Scavengers of hydrogen peroxide or hydroxyl radicals exerted only partial inhibition on the peptide oxidation.

Conclusions. The results of this study are rationalized by the abilities of PAC chelators (i) to extract iron from potential binding sites of the peptides to impair site-specific oxidation, and (ii) to promote the formation of ROS different from the species formed at the peptide metal-binding sites.

KEY WORDS: iron; chelator; oxidation; methionine/histidine.

INTRODUCTION

Proteins and peptides are susceptible towards transition metal-catalyzed oxidation (1–3). With the advent of biotechnological production of therapeutic proteins, such metal-catalyzed oxidation becomes one major concern to the pharmaceutical industry due to the unknown biological activities and half-lives of the oxidized proteins (4). Metals can be present as contamination and/or as intentional additives for some specific manufacturing processes, such as oxidative protein refolding by Cu^{2+} and metal-affinity chromatography. Histidine (His) and methionine (Met) are two of the most susceptible residues (3,5) and have been shown to suffer oxidation in various protein pharmaceuticals such as recombinant relaxin (6) and human growth hormone (hGH) (7,8). Under normal storage conditions, oxidation of hGH occurs predominantly at Met14 (8), which is located close to a metal-binding site composed of His18, His21, and Glu174 (9). One potential rationale would be that the nearby metal-binding site would catalyze Met oxidation through locally formed reactive oxygen species (ROS). Such a possibility is supported by the test of several model peptides that contained neighboring Met and His residues (10).

Metal chelators, such as polyaminocarboxylates (PACs), are commonly perceived as inhibitors of metal-catalyzed oxidation. However, this view has been challenged by the emergence of a number of reports on the catalytic role played by EDTA and similar PACs. For example, EDTA promoted the oxidation of amino acids by the classical Fenton system (H_2O_2/Fe^{2+}) at [EDTA] $\leq$ [Fe^{2+}] (1). Yet the overall literature is non-specific with little rationale behind the results. It seems that the effects of chelators on metal-catalyzed oxidation depend strongly on the nature of the metals, the substrates, and the oxidation mechanisms involved.

The present work investigates the effects of PACs on DTT/Fe^{3+}/O_2-induced oxidation of two model peptides, GGGMGGG and GHGMGGG. Both peptides contain a central oxidation-labile residue, Met. In addition, GHGMGGG has a metal-binding and oxidation-labile residue, His. Our objective here is to demonstrate that PACs will not necessarily protect peptides from oxidation but rather induce significant changes in the oxidation mechanisms, yielding different patterns of peptide oxidation.

Experimental

Materials

The heptapeptides, GGGMGGG and GHGMGGG, were synthesized by standard solid-phase techniques (11) using the Fmoc-protected amino acids obtained from Bachem Bioscience, Inc. The respective sulfoxides were synthesized as described (10). Other chemicals were obtained as follows: dithiothreitol (DTT), $FeCl_3 \cdot 6H_2O$, trifluoroacetic acid (TFA), catalase, superoxide dismutase, NTA, EDDA, EDTA, EGTA, and DTPA from Sigma; sodium phosphate (monobasic and dibasic), H_2O_2 (30% in H_2O), methanol, acetonitrile (ACN), acetone, and isopropanol (i-PrOH) from Fisher Scientific; tetrabutylammonium dihydrogen phosphate (1.0 M in H_2O) from Aldrich; 2,4-dinitrophenylhydrazine (2,4-DNPH) from Eastman Kodak Company.

Reaction Conditions

All reactions were performed at room temperature in 500 μl of aqueous solutions containing 0.4 mM peptide, 2.0 mM DTT, 100 μM $FeCl_3$, 0–200 μM PAC (EDDA, NTA, EGTA,

[1] Department of Pharmaceutical Chemistry, University of Kansas, 2095 Constant Avenue, Lawrence, Kansas 66047.
[2] Amgen Inc., 1840 DeHavilland Drive, Thousand Oaks, CA 91320.
[3] To whom correspondence should be addressed.

ABBREVIATIONS: ACN, acetonitrile; DTPA, diethylenetriaminepentaacetate; DTT, dithiothreitol; EDDA, ethylenediaminediacetate; EDTA, ethylenediaminetetraacetate; EGTA, ethylenebis(oxyethylenenitrilo)tetraacetate; i-PrOH, isopropanol; NTA, nitrilotriacetate; PAC, polyaminocarboxylate; ROS, reactive oxygen species; TFA, trifluoroacetic acid.

0724-8741/96/0600-0931$09.50/0

EDTA, or DTPA), 20 mM sodium phosphate, pH 7.4. DTT and $FeCl_3$ stock solutions were freshly prepared; chelators and $FeCl_3$ solutions were pre-mixed (designated as chelator-Fe^{3+}) unless specified otherwise. Due to its low solubility in the absence of PACs, Fe^{3+} is not present in solution as its free hydrated form, Fe^{3+}_{aq}, but as complexes with the buffer, the peptide, and/or DTT (as discussed in detail in ref. 10). In the presence of chelators, it is important to note that the sequence of addition of the chelators and iron salt significantly affects the nature of the iron complexes formed in the reaction mixture. Despite the thermodynamically favored binding between the PAC chelators and Fe^{3+}, formation of the complexes could be kinetically slow when Fe^{3+} has been complexed with the phosphate buffer of the reaction solution prior to the addition of PAC (as shown in Results). Intermediary species were proposed to form in which the accessibility of the Fe^{3+} centers was hindered (12). DTT was always added last to initiate the reactions. ROS scavengers, if applied, were added before DTT.

HPLC Analysis

The reactions were monitored by RP-HPLC analysis on a Shimadzu 10A HPLC system. Peptides and their oxidation products were separated on an SGE C_{18} column (Nucleosil, 4.6 × 250 mm) and were monitored by UV detection at 214 nm. A linear gradient mobile phase system ran from 95% water, 5% ACN, and 0.023% TFA to 70% water, 30% ACN, and 0.025% TFA over 30 minutes with a flow rate of 1 ml/min. Calibration curves of peptide standard solutions were obtained to calculate the extinction coefficients. The assay was sensitive and reproducible to monitor as low as 1 μM peptide. Oxidation products, including Met sulfoxide, 2-oxo-His, and an N-terminal adduct, were purified by HPLC and characterized by positive FAB-MS and ^{1}H-NMR (see below). The concentrations of these products were calculated using the extinction coefficient of the native peptide since the chromophores monitored were mainly the peptide bond and the imidazole system of His. Final yields were measured at the end of the reactions, i.e. after DTT was completely converted into DTT_{ox}. Chelator-Fe^{3+} complexes and their oxidation products were resolved by ion-pairing RP chromatography according to a slightly modified procedure of Deacon *et al.* (13). A Poros C_{18} perfusion column (4.6 × 150 mm) was used with an isocratic mobile phase of 50 mM tetrabutylammonium phosphate at pH 7.5, and the chelator-Fe^{3+} complexes were monitored by UV detection at 340 nm. In our reactions, chelator-Fe^{3+} is repeatedly reduced to chelator-Fe^{2+} by DTT and oxidized back by O_2. Since the oxidation step proceeds much faster than the reduction step, the calculated steady state concentration of chelator-Fe^{2+} was less than 1% of the total concentration of chelator-Fe^{3+} (see Results). Therefore, it is valid to assume that the chromatographic peak area during the reaction is directly proportional to the chelator-Fe^{3+} concentration.

Analysis of Ammonia

Upon the completion of the reactions, the yield of ammonia was measured by an ammonia-sensitive electrode (Fisher Scientific) coupled to a voltmeter (Orion 420A).

Quantification of Acetone

Acetone formation from isopropanol oxidation was quantified through derivatization with 2,4-DNPH followed by RP-HPLC analysis. An aliquot of 100 μl of 0.1 M 2,4-DNPH (in 1 M HCl) was added to 200 μl reaction mixture, and the reaction was stirred at room temperature for 10 minutes. The hydrazone derivative was then extracted with 50 μl hexane and analyzed by RP-HPLC with UV detection at 345 nm. An SGE C_{18} column (nucleosil; 4.6 × 250 mm) was employed, and the mobile phase was a 1:1 (v/v) mixture of ACN and H_2O. Standards made from HPLC grade acetone were derivatized and analyzed in the same fashion. The detection limit was 1 μM.

RESULTS

Effect of EDTA on the Peptide Oxidation by DTT/Fe^{3+}/O_2

Product Formation

The oxidation of GGGMGGG and GHGMGGG by DTT/Fe^{3+}/O_2 alone at pH 7.4 yielded predominantly Met sulfoxide (see Table I). This is representatively shown for the oxidation of GHGMGGG in Figure 1. The sulfoxides were identified and quantified by comparison with the authentic standards. Furthermore, their identities were confirmed by FAB-MS and ^{1}H-NMR. For both sulfoxides, the mass spectra indicated a gain of 16 amu as compared to the starting peptides. ^{1}H-NMR then confirmed that oxygen was introduced at the methionine residue, showing a singlet at 2.75 ppm for the ε-methyl group. In addition, there were significant yields for a peptide adduct **1a** and its oxidized form **1b** (as shown in Figure 1). Mass spectrometric analysis of **1a** suggests that it represents a Schiff base formed via the reaction of the peptide N-terminus with $CH_3C(=O)CH(OH)CH_2SH$, a Potential oxidation product of DTT (14). 500MHz ^{1}H-NMR spectra of **1a** displays essentially all the same amino acid resonances of GHGMGGG, indicating that no amino acid side chain had been modified. The product **1b** could be directly obtained by oxidation of **1a** with H_2O_2. Since **1a** and **1b** do not represent products from the direct oxidation of amino acid side chains of the native peptide, we did not further study their mechanisms of formation except that we had to monitor them to account for the loss of starting peptides.

Upon the addition of 20–200 μM EDTA to the DTT/Fe^{3+}/O_2 system (designated as DTT/EDTA-Fe^{3+}/O_2), the peptides still underwent significant oxidation. However, Met sulfoxide was no longer the major product at [EDTA] ≥ [Fe^{3+}], accounting for no more than 30% of the peptide loss (Table I). The oxidation of the His-containing peptide GHGMGGG to 2-oxo-His increased significantly (for all PACs except EGTA and DTPA), displaying yields that are comparable to the Met sulfoxide yields (Figure 1, Table II). 2-oxo-His refers to the peptide product in which the imidazole side chain of His is oxidized to 2-oxo-imidazole (Figure 2). The characterization of 2-oxo-His was achieved by positive FAB-MS/MS and 500MHz ^{1}H-NMR. Positive FAB-MS revealed a molecular ion of $[M + H]^+ = 588$, which is 16 amu higher than the parent peptide ion. In order to gain higher mass spectrometric sensitivity, the HPLC fraction of 2-oxo-His was lyophilized and derivatized to a C-terminal hexyl ester with $C_6H_{13}OH$. The expected molecular ion of $[M + H]^+ = 672$ for $GH(O)GMGGG(CO_2C_6H_{13})$ was then

Table I. The Effect of EDTA on DTT/Fe^{3+}/O_2 Induced Peptide Oxidation and Sulfoxide Yield[a]

Peptide	−EDTA[b] sulfoxide μM	−EDTA[b] −peptide[d] μM	−EDTA[b] sulfoxide/−peptide	+EDTA[c] sulfoxide μM	+EDTA[c] −peptide[d] μM	+EDTA[c] sulfoxide/−peptide	EDTA inhibition sulfoxide	EDTA inhibition −peptide[d]
GGGMGGG	124 ± 7	179 ± 13	69.3%	24 ± 1	95 ± 2	25.3%	81%	47%
GHGMGGG	122 ± 12	183 ± 10	66.7%	17 ± 3	151 ± 12	11.3%	86%	17%

[a] Sulfoxide yields and peptide consumptions were measured after completion of the reactions, i.e. when DTT was completely consumed.
[b] Reaction conditions: 0.4 mM peptide, 2 mM DTT, 100 μM Fe^{3+}, 20 mM sodium phosphate buffer, pH 7.4.
[c] Reaction conditions: same as (b) plus 100 μM EDTA.
[d] Values represent the consumption of the peptide.

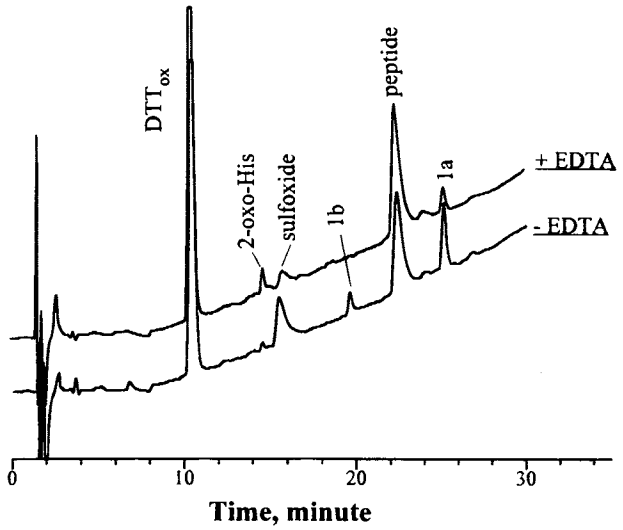

Fig. 1. Representative chromatograms obtained upon the completion of GHGMGGG oxidation reactions in the presence or absence of EDTA, respectively. Initial reaction conditions: 0.4 mM GHGMGGG, 2 mM DTT, 100 μM EDTA-$FeCl_3$ or $FeCl_3$, 20 mM sodium phosphate buffer at pH 7.4. Analytes were separated on an SGE C_{18} column and monitored by UV detection at 214 nm. Linear gradient program: 5% ACN, 0.023% TFA to 30% ACN, 0.025% TFA over 30 minutes; flow rate: 1.0 ml/min.

observed by positive FAB-MS. MS/MS experiments of this molecular ion led to the identification of the characteristic fragments B_2(m/e = 211) and B_3(m/e = 268), which are indicative for the incorporation of oxygen into the His residue. The ^{1}H-NMR spectrum of the 2-oxo-His fraction is displayed in Figure 2. The clean singlet at 2.1 ppm (proton **c**) together with the absence of signals at 2.5–2.7 ppm (region **b**) indicate an unoxidized Met residue. On the other hand, the resonance at 6.35 ppm (proton **a**; singlet) most likely corresponds to the 2-oxo-imidazole C_4-H of 2-oxo-His, in analogy to the signal at 6.0 ppm obtained earlier by Kawakishi and Uchida for N-benzoyl-2-oxo-His (15). The two less intense resonance recorded at 7.3 ppm (singlet) and 8.65 ppm (singlet) may correspond to His imidazole protons, possibly introduced through a contamination of our 2-oxo-His HPLC fraction by the closely eluting sulfoxide product.

Often His oxidation has been reported to yield Asn and Asp (16,17). Subsequent to the oxidation of GHGMGGG, we could not reveal any significant (≥1 μM) formation of GNGMGGG(t_r = 11.9 min.) or GDGMGGG (t_r = 12.8 min.).

Ammonia, which can form through the oxidation and subsequent N-dealkylation of a peptide N-terminus, was detected. The final yields of ammonia for GGGMGGG and GHGMGGG oxidation by DTT/EDTA-Fe^{3+}/O_2 were 8 ± 0.1 μM and 15 ± 0.1 μM, respectively.

From Table II, we derive that in the presence of PACs the final yields of identified products only account for ca. 43–55%

Table II. The Effects of the PACs on the DTT/Fe^{3+}/O_2 Induced Oxidation of GHGMGGG[a]

Chelator	logK (Fe^{3+})[b]	logK (Fe^{2+})[b]	2-oxo-His μM	sulfoxide μM	ammonia μM	1a μM	−GHGMGGG[c] μM	Products/−GHGMGGG[d]
No Chelator	—	—	6 ± 2	122 ± 12	0	35 ± 1	183 ± 10	89.1%
NTA	16	8	19 ± 1	17 ± 1	n.d.[e]	23 ± 1	138 ± 10	42.8%
EDDA	17	10	18 ± 1	17 ± 1	n.d.	21 ± 1	130 ± 2	43.1%
EGTA	21	12	7 ± 1	69 ± 6	n.d.	29 ± 3	191 ± 9	55.0%
EDTA	25	14	19 ± 1	17 ± 3	15 ± 1	17 ± 2	151 ± 12	35.1%
DTPA	28	16	12 ± 1	54 ± 2	n.d.	37 ± 1	188 ± 1	54.8%

[a] Reaction conditions: 0.4 mM GHGMGGG, 2 mM DTT, 100 μM chelator-Fe^{3+}, 20 mM sodium phosphate buffer, pH 7.4. All yields were measured after complete oxidation of DTT.
[b] K represents the stability constant for 1:1 chelator:iron complex (Ref. 24).
[c] Values represent the consumption of peptides.
[d] Products include only the total yield of 2-oxo-His, **1a**, and sulfoxide.
[e] "n.d." stands for "not determined."

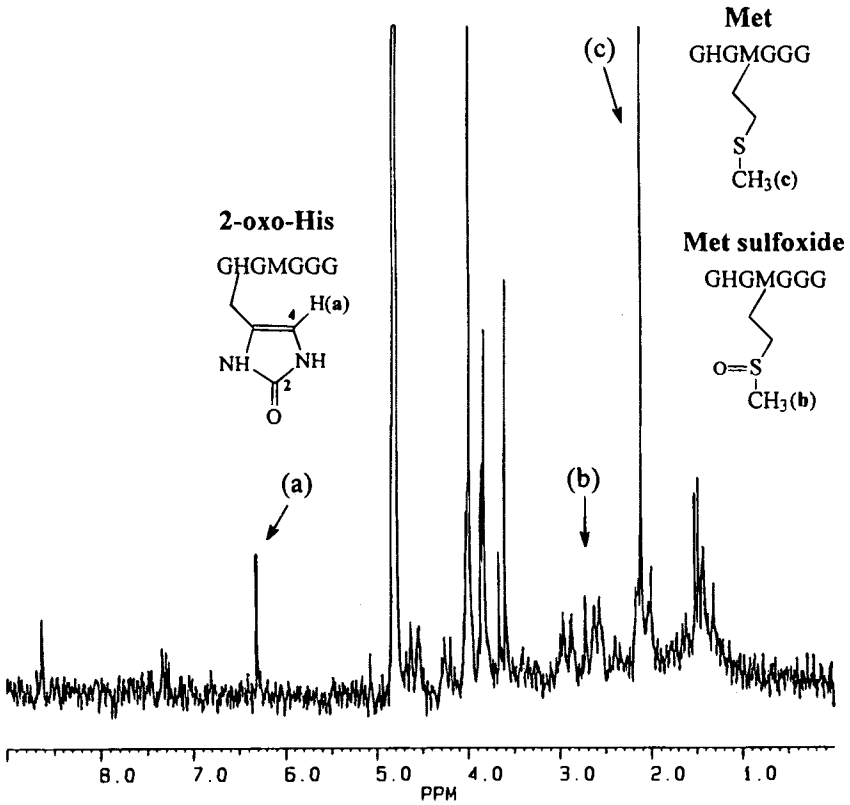

Fig. 2. ^{1}H-NMR spectrum (500MHz) of the HPLC fraction denoted as 2-oxo-His in Figure 1.

of the lost peptide, in contrast to ca. 89% obtained in the reaction without any chelators. This implies a rather non-selective nature of the ROS generated in the chelator-containing systems and bears important mechanistic implications. It should be stated that owing to the potential HO•-like nature of our oxidizing intermediate, a significant fraction of products may originate from hydrogen abstraction from C_α-H bonds along the peptide chain (18). This route will result in a manifold of potential elimination and fragmentation processes which may account for the poor material balance in the chelator-containing systems.

By employing ion-pairing RP chromatography, EDTA itself was observed to undergo degradation in the reactions driven by DTT/EDTA-Fe^{3+}/O_2, consistent with earlier observations that EDTA degraded during metal-catalyzed oxidation involving EDTA-Fe^{3+} (19).

Kinetics

Figures 3a and 3b compare the oxidation kinetics of DTT and GHGMGGG by three oxidizing systems, namely DTT/Fe^{3+}/O_2, DTT/EDTA-Fe^{3+}/O_2 (EDTA and $FeCl_3$ pre-mixed), and DTT/EDTA/Fe^{3+}/O_2 (EDTA and $FeCl_3$ added separately).

In the absence of chelators, the oxidation of DTT and peptide followed approximately first order kinetics after a short induction period (see ref. 10 for a rationale of the induction period). In the presence of pre-mixed EDTA-Fe^{3+}, the oxidation of both DTT and peptide accelerated and followed apparent zero-order kinetics. When $FeCl_3$ and EDTA were added separately to the reaction solution, there was a significant lag period before the oxidation of DTT and peptide accelerated to a rate comparable to the pre-mixed EDTA-Fe^{3+}-catalyzed process. Nevertheless, the final product yields and peptide consumption showed no statistically significant differences regardless whether the reaction was performed with EDTA-Fe^{3+} or EDTA/Fe^{3+}. This observation implies the existence of a kinetic barrier in the DTT/EDTA/Fe^{3+}/O_2 system, possibly caused by the sterically hindered accessibility of Fe^{3+} within an intermediary ternary complex [EDTA-Fe^{3+}-phosphate] (12).

Figure 3c indicates that during DTT/EDTA-Fe^{3+}/O_2-catalyzed oxidation reaction, the degradation of the EDTA-Fe^{3+} complex, measured over one half-life, also followed zero-order kinetics.

Effects of ROS Scavengers on GHGMGGG Oxidation by DTT/EDTA-Fe^{3+}/O_2

To elucidate the nature of the ROS involved in EDTA-Fe^{3+}-catalyzed oxidation of the peptides, selective ROS scavengers were applied to the oxidation reactions of GHGMGGG (0.4 mM GHGMGGG, 2 mM DTT, 100 μM EDTA-Fe^{3+}, 20 mM sodium phosphate, pH 7.4).

Effect of Superoxide Dismutase

The addition of superoxide dismutase up to 840 U/ml did not affect the oxidation of GHGMGGG by DTT/EDTA-Fe^{3+}/O_2. We conclude that freely diffusable superoxide anion radicals do not directly oxidize the peptide.

Effect of Isopropanol

Isopropanol (i-PrOH) efficiently scavenges HO• (20) and HO•-like ROS (21). Figure 4a shows the effect of increasing

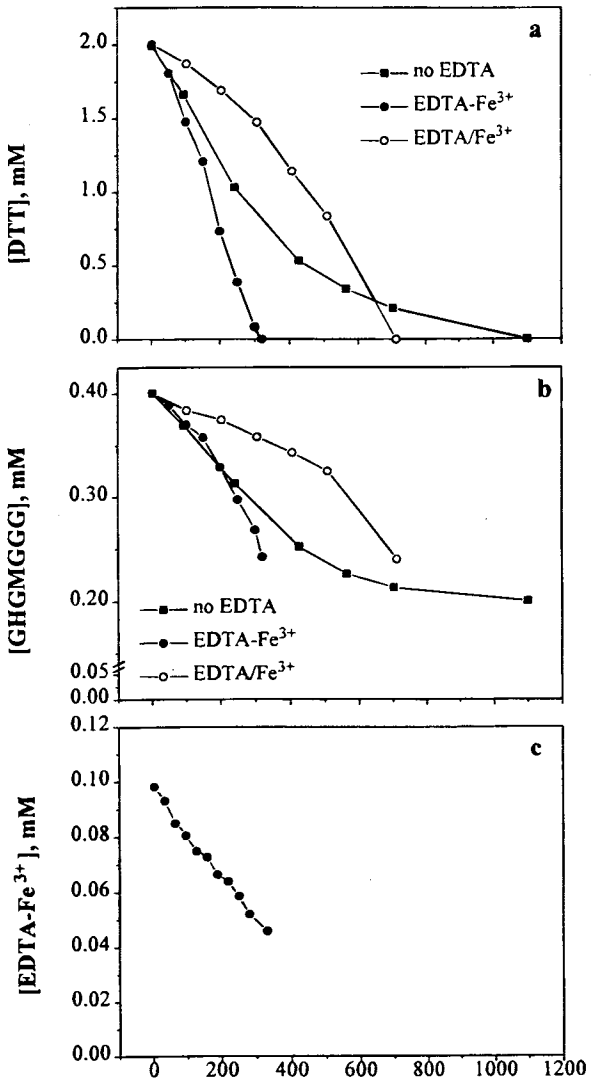

Fig. 3. Oxidation kinetics of (**a**) DTT and (**b**) GHGMGGG catalyzed by the following systems: Fe^{3+} (no EDTA), EDTA/Fe^{3+} (Fe^{3+} and EDTA sequentially added), and EDTA-Fe^{3+} (Fe^{3+} and EDTA premixed). Reaction conditions: 0.4 mM GHGMGGG, 2 mM DTT, 100 μM of either $FeCl_3$, EDTA/$FeCl_3$, or EDTA-$FeCl_3$, 20 mM phosphate buffer, pH 7.4. (**c**) Oxidation of EDTA-Fe^{3+} in a reaction of 0.4 mM GHGMGGG, 2 mM DTT, 100 μM EDTA-$FeCl_3$, 20 mM phosphate buffer at pH 7.4.

i-PrOH concentration on the oxidation of GHGMGGG. The presence of 0.2 M i-PrOH successfully inhibited 89% of the 2-oxo-His formation but only 41% of the sulfoxide formation. This may suggest that HO° (or a HO°-like ROS) is responsible for the 2-oxo-His formation. The sulfoxide formation was not further suppressed by the addition of up to 2.0 M i-PrOH. The overall peptide consumption was protected maximally to an extent of 90% but never 100%, as [i-PrOH] was increased from 0.1 to 2.0 M.

The reaction of i-PrOH and HO° in oxygen-containing solution yields acetone as a characteristic product. In order to demonstrate that the observed inhibitory effect of i-PrOH was not due to any physical solvent effect but rather the scavenging of HO° type ROS, we determined the formation of acetone in the same reaction. A continuous linear formation of acetone was observed as a function of time. Due to the as yet unknown nature of the ROS, the yield of acetone should not be taken as the absolute ROS concentration.

Isopropanol reacts with HO° with $k = 1.9 \times 10^9\ M^{-1}s^{-1}$ (20). Theoretically, if HO° would be responsible for the peptide oxidation by DTT/EDTA-Fe^{3+}/O_2, competition kinetics predict that 1 M i-PrOH should be adequate to completely suppress the peptide oxidation, considering all possible competing pathways in the reaction, i.e. the reactions of HO° with DTT ($k = 1.5 \times 10^{10}\ M^{-1}s^{-1}$), EDTA-$Fe^{3+}$ ($k = 1.1 \times 10^9\ M^{-1}s^{-1}$), EDTA-$Fe^{2+}$ ($k = 7.5 \times 10^9\ M^{-1}s^{-1}$), Met ($k = 8.3 \times 10^9\ M^{-1}s^{-1}$), and His ($k = 5 \times 10^9\ M^{-1}s^{-1}$), (all rate constants from ref. 20). An upper limit of the steady state concentration of EDTA-Fe^{2+}, $[EDTA\text{-}Fe^{2+}]_{ss}$, was estimated to be 5×10^{-8} M based on the following equations:

$$-\frac{d[EDTA - Fe^{3+}]}{dt} = k_1[DTT][EDTA - Fe^{3+}] - k_2[EDTA - Fe^{2+}][O_2] \quad (k_2 \cong 10^4\ M^{-1}s^{-1};\ \text{ref. 22})$$

$$k_1[DTT][EDTA - Fe^{3+}] \approx -\frac{d[DTT]}{dt} \approx 1.12 \times 10^{-7}\ M/s$$

(calculated from Figure 3a)

The fact that even 2 M i-PrOH failed to completely protect the peptide, especially the Met sulfoxide formation, implicates that Met sulfoxide formation was not caused solely by HO° present in the bulk solution. The observed suppression of 2-oxo-His formation by i-PrOH at concentrations smaller than 0.5 M could well be rationalized by the participation of free HO° in the oxidation process but also leaves room for the contribution of HO°-like species such as $Fe^{IV}{=}O$ or $Fe^{V}{=}O$.

Effect of Catalase

If H_2O_2 would be responsible for the peptide oxidation, then 200 U/ml catalase should display a complete inhibition of the peptide oxidation, based on the reaction rates of H_2O_2 with the competing substrates at maximum concentrations: DTT ($k = 7\ M^{-1}s^{-1}$; ref. 23a), Met ($k = 10^{-2}\ M^{-1}s^{-1}$; ref. 23b), catalase ($k = 1.5 \times 10^6\ M^{-1}s^{-1}$; ref. 23c), EDTA-$Fe^{2+}$ ($k = 1.4 \times 10^4\ M^{-1}s^{-1}$; ref. 21). Again, $[EDTA\text{-}Fe^{2+}]_{ss}$ is estimated to be 5×10^{-8} M (see above). As shown in Figure 4b, the addition of 200 U/ml catalase to the reaction systems only negligibly inhibited the oxidation of GHGMGGG by DTT/EDTA-Fe^{3+}/O_2. For each experiment, the catalase activity at the end of the reaction was confirmed as described before (10). Heat-denatured catalase had no effect on the oxidation reactions, indicating that the protein skeleton *per se* is not a competing substrate for ROS. Importantly, the yields of both sulfoxide and 2-oxo-His were equally sensitive to catalase (Figure 4b). In contrast, the yield of 2-oxo-His was more sensitive to the inhibition by i-PrOH than the yield of sulfoxide (Figure 4a).

Effects of i-PrOH and Catalase on the Oxidation Kinetics

Based on the finding that both i-PrOH and catalase can inhibit the peptide oxidation, we conclude that there are more

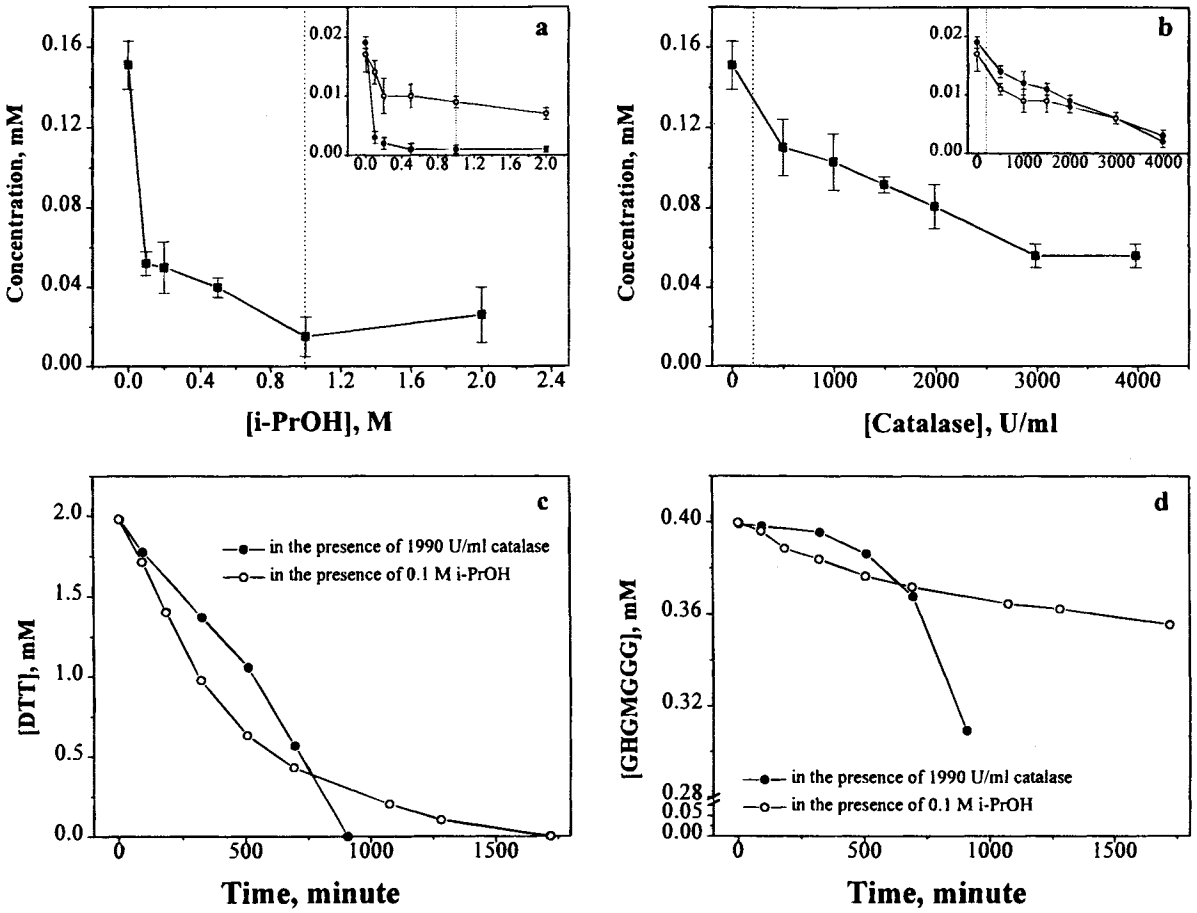

Fig. 4. Effects of **(a)** 0.1–2.0 M i-PrOH and **(b)** 550-3980 U/ml catalase on the *final yields* of GHGMGGG oxidation by DTT/EDTA-Fe^{3+}/O_2 (0.4 mM GHGMGGG, 2 mM DTT, 100 μM EDTA-Fe^{3+}, 20 mM phosphate buffer at pH 7.4). (■) GHGMGGG consumption; (●) 2-oxo-His yield; (○) sulfoxide yield. The dotted lines indicate the theoretical concentrations at which catalase or i-PrOH should exhibit 100% inhibition of the peptide oxidation. Effects of i-PrOH (0.1 M) and catalase (1990 U/ml) on the *oxidation kinetics* of **(c)** DTT and **(d)** GHGMGGG.

than one ROS directly involved in the peptide oxidation by the DTT/EDTA-Fe^{3+}/O_2 system. Additional information on the relationship among the ROS can be extracted from the effects of i-PrOH and catalase on the oxidation kinetics of DTT and peptide. Figures 4c and 4d compare the oxidation kinetics representatively for GHGMGGG in the presence of either 0.1 M i-PrOH or 1990 U/ml catalase. In the presence of i-PrOH, the oxidation of both DTT and peptide followed first-order kinetics similar to the reaction driven by DTT/Fe^{3+}/O_2 in the absence of EDTA. Apparently, i-PrOH affects a process that is responsible for the observed zero-order kinetics in the DTT/EDTA-Fe^{3+}/O_2 system. Potentially this may relate to the decomposition of the chelator which results in the formation of new chelating species in the course of the oxidation reaction. The presence of catalase slowed down the oxidation of both DTT and peptide, but it did not significantly change the overall rate law of oxidation.

Effects of Other Chelators on the Oxidation of GHGMGGG by DTT/Fe^{3+}/O_2

The oxidation of GHGMGGG by DTT/Fe^{3+}/O_2 was representatively investigated in the presence of EDDA, NTA, EGTA, and DTPA, selected to cover a wide range of binding affinities for Fe^{2+} and Fe^{3+} (see values in Table II) (24). None of the chelators was able to inhibit the oxidation of GHGMGGG. Again, all chelators were observed to suffer degradation. As shown in Table II, EDDA and NTA exerted similar effects as EDTA. Moreover, they promoted the apparent zero-order oxidation of DTT and peptide to even higher rates as compared to EDTA (data not shown). On the other hand, the presence of EGTA or DTPA slowed down the oxidation, rendering first-order kinetics. These slower kinetics were paralleled by higher consumption of the peptide and a more selective product distribution consisting of a larger fraction of Met sulfoxide.

DISCUSSION

In the absence of PAC chelators, the DTT/Fe^{3+}/O_2 system promotes the oxidation of Met in peptides in a site-specific manner (10). Such site-specific processes are impaired through the complexation of Fe^{3+} by PAC chelators. Nevertheless, the presence of PACs results in an accelerated peptide oxidation. The crystal structure of EDTA-Fe^{3+} displays seven coordination sites of the central Fe^{3+}, six of them coordinating with EDTA and one with a H_2O molecule (25). This water ligand is substitution-

labile and should easily be replaced by other ligands such as the mercapto groups of DTT. Thus, redox active molecules can have access to the Fe^{3+} center which serves as a basis to rationalize the catalytic activity of EDTA-Fe^{3+} and other PAC-Fe^{3+} complexes with six- or less dentate chelators. However, the catalytic activities of DTPA-Fe^{3+} and EGTA-Fe^{3+} cannot be rationalized that easily and their mechanisms may be different as compared to the other employed chelators (indicated also by the significant different product stoichiometry of the DTPA- or EGTA-containing system).

From the product distribution and the differential effects of the ROS scavengers, we conclude that more than one specific species are involved in the peptide oxidation. For example, neither catalase nor i-PrOH were able to completely inhibit peptide oxidation at concentrations theoretically sufficient based on the hypothetical assumption that either solely HO° or solely H_2O_2 was involved in peptide oxidation. Clearly, the species yielding Met sulfoxide cannot be HO° alone as we have shown that the reaction of HO° with organic sulfides does not efficiently yield sulfoxide in air-saturated reaction systems (26). This becomes evident also from the fact that the HO° scavenger i-PrOH neither completely inhibits sulfoxide formation nor promotes stoichiometric sulfoxide formation (for a more detailed consideration of expected sulfoxide yields and stoichiometries in the presence of alcohols, see ref. 10). On the other hand, the low steady-state concentrations of EDTA-Fe^{2+} in our system can react with H_2O_2 to yield $[EDTA\text{-}Fe^{II}\text{-}H_2O_2]^{2-}$ (21) which can eliminate H_2O or OH^- to yield $[EDTA\text{-}Fe^{IV} = O]^{2-}$ or $[EDTA\text{-}Fe^{IV}\text{-}OH]^-$, respectively (27). The reaction of the latter species with Met-containing peptides produces significant yields of Met sulfoxide even in the presence of a large excess of i-PrOH (28). Besides that, the direct reaction of H_2O_2 with Met yields Met sulfoxide stoichiometrically.

The oxidation of His to 2-oxo-His appears to be carried out by a species of HO°-like reactivity. This can be free HO°, generated by decomposition of $[EDTA\text{-}Fe^{II}\text{-}H_2O_2]^{2-}$ into $[EDTA\text{-}Fe^{III}\text{-}OH]^-$ and HO°, as we have shown that $[EDTA\text{-}Fe^{II}\text{-}H_2O_2]^{2-}$ generates a species which reacts with Met-containing peptides in a HO°-like manner (28). Further evidence for the involvement of HO° or an alike species is pertinent through the decomposition of the PACs during the oxidation process (29) and the formation of ammonia. On the other hand, we may also expect that either $[EDTA\text{-}Fe^{IV} = O]^{2-}$ or $[EDTA\text{-}Fe^{IV}\text{-}OH]^-$ can directly react with His. These latter possibilities will be examined further in the future.

CONCLUSIONS

Site-specific oxidation of Met by DTT/Fe^{3+}/O_2 was observed in the absence of metal chelators. The addition of polyaminocarboxylate chelators resulted in multiple reactive oxygen species in the bulk solution, leading to the oxidation of various target sites in peptides, including His, Met and the N-terminus. Polyaminocarboxylate chelators should, therefore, be used with caution in protein formulations as they may have adverse rather than protective effects.

ACKNOWLEDGMENTS

The authors would like to thank Drs. David Vander Velde, Martha Morton, and Todd D. Williams for the assistance in product identification by NMR and Mass spectroscopy. Financial support was provided by the Association for International Cancer Research (AICR).

REFERENCES

1. E. R. Stadtman. Oxidation of free amino acids and amino acid residues in proteins by radiolysis and by metal-catalyzed reactions. *Annu. Rev. Biochem.* **62**:797–821 (1993).
2. E. R. Stadtman and C. N. Oliver. Metal-catalyzed oxidation of proteins. *J. Biol. Chem.* **266**:2005–2008 (1991).
3. E. R. Stadtman. Metal-ion catalyzed oxidation of proteins: Biochemical mechanism and biological consequences. *Free Rad. Biol. Med.* **9**:315–325 (1990).
4. M. C. Manning, K. Patel, and R. T. Borchardt. Stability of protein pharmaceuticals. *Pharm. Res.* **6**:903–918 (1989).
5. W. Vogt. Oxidation of methionyl residues in proteins: tools, targets, and reversal. *Free Rad. Biol. Med.* **18**:93–105 (1995).
6. S. Li, T. Nguyen, C. Schöneich, and R. T. Borchardt. Aggregation and precipitation of human relaxin induced by metal-catalyzed oxidation. *Biochemistry* **34**:5762–5772 (1995).
7. R. Pearlman and T. Nguyen. Pharmaceutics of protein drugs. *J. Pharm. Pharmacol.* **44(suppl.1)**:178–185 (1992).
8. G. W. Becker, P. M. Tackitt, W. W. Bromer, D. S. Lefeber, and R. M. Riggin. Isolation and characterization of a sulfoxide and a desamido derivative of biosynthetic human growth hormone. *Biotechnol. Appl. Biochem.* **10**:326–337 (1988).
9. B. C. Cunningham, M. G. Mulkerrin, J. A. Wells. Dimerization of human growth hormone by zinc. *Science* **253**:545–548 (1991).
10. Ch. Schöneich, F. Zhao, G. S. Wilson, and R. T. Borchardt. Iron-thiolate induced oxidation of methionine to methionine sulfoxide in small model peptides. Intramolecular catalysis by histidine. *Biochim. Biophys. Acta* **1158**:307–322 (1993).
11. E. Atherton and R. C. Sheppard. *Solid phase peptide synthesis. A practical approach.* IRL Press at Oxford University Press. 1989.
12. G. A. Elgavish and J. Granot. Enhancement of ^{31}P relaxation rates of orthophosphate and ATP in the presence of EDTA. Evidence for EDTA-Fe(III)-phosphate ternary complexes. *J. Magn. Reson.* **36**:147–150 (1979).
13. M. Deacon, M. R. Smyth, and L. G. M. T. Tuinstra. Chromatographic separations of metal chelates present in commercial fertilizers. II. Development of an ion-pair chromatographic separation for the simultaneous determination of Fe(III) chelates of EDTA, DTPA, HEEDTA, EDDHA and EDDHMA, and the Cu(II), Zn(II) and Mn(II) chelates of EDTA. *J. Chromatog. A* **659**:349–357 (1994).
14. M. S. Akhlaq and C. v. Sonntag. Free-radical-induced elimination of H_2S from dithiothreitol. A chain reaction. *J. Am. Chem. Soc.* **108**:3542–3544 (1986).
15. K. Uchida and S. Kawakishi. Selective oxidation of imidazole ring in histidine residues by the ascorbic acid-copper ion system. *Biochem. Biophys. Res. Commun.* **138**:659–665 (1986).
16. R. L. Levine. Oxidation modification of glutamine synthase. *J. Biol. Chem.* **258**:11823–11827 (1983).
17. R. T. Dean, S. P. Wolff, and M. A. McElligott. Histidine and proline are important sites of free radical damage to proteins. *Free Rad. Res. Comms.* **7**:97–103 (1989).
18. W. M. Garrison. Reaction mechanisms in the radiolysis of peptides, polypeptides, and proteins. *Chem. Rev.* **87**:381–398 (1987).
19. K. C. Francis, D. Cummins and J. Oakes. Kinetics and structural investigations of $[Fe^{III}(edta)]$-[edta=ethylenediaminetetra-acetate(4-)] catalyzed decomposition of hydrogen peroxide. *J. Chem. Soc. Dalton Trans.* 493–501 (1985).
20. G. V. Buxton, C. L. Greenstock, W. P. Helman, and A. B. Ross. Critical review of rate constants for reactions of hydrated electrons, hydrogen atoms and hydroxyl radicals in aqueous solution. *J. Phys. Chem. Ref. Data* **17**:513–886 (1988).
21. J. D. Rush and W. H. Koppenol. The reaction between ferrous polyaminocarboxylate complexes and hydrogen peroxide: an investigation of the reaction intermediates by stopped flow spectrophotometry. *J. Inorg. Biochem.* **29**:199–215 (1987).
22. M. A. Miller, D. Bandyopadyay, J. M. Mauro, T. G. Traylor, and J. Kraut. Reaction of ferrous cytochrome *c* peroxidase with dioxygen: site-directed mutagenesis provides evidence for rapid

reduction of dioxygen by intramolecular electron transfer from the compound I radical site. *Biochemistry* **31**:1992 (1992).
23. (a) N. Zhang, H. P. Schuchmann, and C. von Sonntag. The reaction of superoxide radicalanion with dithiothreitol—a chain process. *J. Phys. Chem.* **95**:4718–4722 (1991). (b) P. K. Sysak, C. S. Foote, and Ta-Y. Ching. Chemistry of singlet oxygen-XXV. Photooxygenation of methionine. *Photochem. Photobiol.* **26**:19–27 (1977) (c) calculated from catalase activity defined by Sigma.
24. L. G. Sillèn. *Stability constants of metal ion complexes.* Chemical Society. London. 1964.
25. J. L. Hoard, M. Lind, and J. V. Silverton. The stereochemistry of the ethylenediamine-tetraacetatoaquoferrate(III) ion. *J. Am. Chem. Soc.* **83**:2770–2771 (1961).
26. Ch. Schöneich, A. Aced, and K.-D. Asmus. Mechanism of oxidation of aliphatic thioethers to sulfoxides by hydroxyl radical. The importance of molecular oxygen. *J. Am. Chem. Soc.* **115**:11376–11383 (1993).
27. S. Rahhal and H. W. Richter. Reduction of hydrogen peroxide by the ferrous iron chelate of diethylenetriamin-N,N,N′,N″,N″-pentaacetate. *J. Am. Chem. Soc.* **110**:3126–3133 (1988).
28. Ch. Schöneich and J. Yang. Oxidation of methionine peptides by Fenton systems: The importance of peptide sequence, neighboring groups, and EDTA. *J. Chem. Soc. Perkin Trans II* (1996), in press.
29. J. D. Rush and W. H. Koppenol. Reactions of Fe^{II}nta and Fe^{II}edda with hydrogen peroxide. *J. Am. Chem. Soc.* **110**:4957–4963 (1988).